

DISCOVERY AND CHARACTERIZATION OF WIDE BINARY SYSTEMS WITH A VERY LOW MASS COMPONENT

Frédérique Baron¹, David Lafrenière¹, Étienne Artigau¹, René Doyon¹, Jonathan Gagné¹,
Cassy L. Davison², Lison Malo³, Jasmin Robert¹, Daniel Nadeau¹, and Céline Reylé⁴
¹ *Département de Physique, Université de Montréal, C.P. 6128 Succ. Centre-ville, Montréal, Qc H3C 3J7, Canada*

² *Department of Physics and Astronomy, Georgia State University, Atlanta, GA 30303, USA*

³ *Canada-France-Hawaii Telescope, 65-1238 Mamalahoa Hwy, Kamuela, HI 96743, USA*

⁴ *Institut Utinam, CNRS UMR6213, Université de Franche-Comté, OSU THETA Franche-Comté-Bourgogne, Observatoire de Besançon, BP 1615, 25010 Besançon Cedex, France*

ABSTRACT

We report the discovery of 14 low-mass binary systems containing mid-M to mid-L dwarf companions with separations larger than 250 AU. We also report the independent discovery of 9 other systems with similar characteristics that were recently discovered in other studies. We have identified these systems by searching for common proper motion sources in the vicinity of known high proper motion stars, based on a cross-correlation of wide area near-infrared surveys (2MASS, SDSS, and SIMP). An astrometric follow-up, for common proper motion confirmation, was made with SIMON and/or CPAPIR at the OMM 1.6 m and CTIO 1.5 m telescopes for all the candidates identified. A spectroscopic follow-up was also made with GMOS or GNIRS at Gemini to determine the spectral types of 11 of our newly identified companions and 10 of our primaries. Statistical arguments are provided to show that all of the systems we report here are very likely to be physical binaries. One of the new systems reported features a brown dwarf companion: LSPM J1259+1001 (M5) has an L4.5 (2M1259+1001) companion at ~ 340 AU. This brown dwarf was previously unknown. Seven other systems have a companion of spectral type L0–L1 at a separation in the 250–7500 AU range. Our sample includes 14 systems with a mass ratio below 0.3.

Subject headings: binaries: general — stars: low-mass, brown dwarfs

1. INTRODUCTION

In the last two decades, the search for low-mass stars and brown dwarfs has intensified with the advent of wide area surveys such as 2MASS (Cutri et al. 2003), DENIS (Epchtein et al. 1999), SDSS (Ahn et al. 2012), UKIDSS (Lawrence et al. 2007), and more recently WISE (Cutri & et al. 2012). In addition, a handful of surveys were aimed at finding nearby binary systems including low mass stars such as the surveys of Reid & Gizis (1997) and Reid et al. (2001) for ex-

ample. Dhital et al. (2010) assembled the SLoW-PoKES catalog which contains 1342 binary systems with a projected separation of $\gtrsim 500$ AU, in which one of the components is a mid-K to mid-M dwarf. Numerous wide binary systems have also been discovered individually. Of all the systems known, very few have a separation larger than 7000 AU. The system composed of NLTT 20346 (an M5V and M6V binary) and 2MASS J0850359+105716 (an L6 dwarf) is one of these, with a separation of 7700 AU (Radigan et al. 2009), while Konigstuhl 3 A-BC (Faherty et al. 2011), a hierarchical system composed of an F8V orbited by an M8V and L3 binary, has a separa-

¹baron@astro.umontreal.ca

tion of 12 000 AU.

An interest of binary systems is that both components share the same age and metallicity. For systems comprising an M dwarf companion for example, this can help calibrate the metallicity scale for this type of star (Bonfils et al. 2005). The components of wide visual binaries can also be studied in detail individually using seeing-limited instruments, making their characterization much easier. Additionally, the evolution of each component of a wide binary system has not been influenced by the other component, and both can be viewed as an “isolated” star.

The discovery of numerous low-mass stars and brown dwarfs has led to a growing interest in understanding the formation mechanism of these objects whose masses are below the typical Jeans mass in a molecular cloud (Meyer et al. 2000), and numerous hypotheses about their origin have been formulated over the years. Binary systems containing a low mass component provide a good tool for attempting to discriminate between the various possibilities, as their properties (e.g., separations, mass ratios) may be affected differently by different processes (Duchêne & Kraus 2013). Wide binary systems with separation larger than hundreds of AU are of particular interest for this purpose as, being more weakly gravitationally bound and spanning sizes larger than typical protostellar disks, they bring additional and perhaps more stringent constraints on the underlying formation processes.

In this article, we report the discovery of 14 new binary systems that all have a component with a spectral type later than M6 and a separation larger than 250 AU. We also recovered nine previously known binaries with similar characteristics. Section 2 details our archival search for wide binaries and the identification of our candidates, while Section 3 describes the follow-up photometry and the calculations of the proper motion. The spectroscopic follow-up as well as the results extracted from these data are explained in Section 4. The probability of random alignment has been calculated for each system and is presented in Section 5. A short discussion is presented in section 6. Our results are summarized in section 7.

2. SEARCH AND IDENTIFICATION OF THE CANDIDATE COMPANIONS

2.1. Sample

We searched for new binary systems comprising a low-mass component through common proper motion based on multi-epoch wide area near-infrared surveys. As a starting point for potential primary stars, we considered the NLTT (Salim & Gould 2003) and LSPM (Lépine 2005) catalogs which include stars with proper motions larger than 0.18 mas yr^{-1} and 0.15 mas yr^{-1} , respectively. We retained only the stars with a relative proper motion measurement error of less than 30%. The large and precise proper motions of these stars are useful to limit the number of false positives, i.e., common proper motion between two sources resulting from chance or measurement errors. To calculate the proper motion of the sources in the vicinity of these target stars, we compared the 2MASS PSC data (Cutri et al. 2003) to data from the SDSS (Adelman-McCarthy et al. 2008) and/or the SIMP (Artigau et al. 2009) surveys. Of the roughly 60,000 stars included in the NLTT and LSPM catalogs, about 25,000 have accurate proper motion measurements and were observed by SIMP or SDSS; those constitute our initial sample. Target baseline’s between the SDSS/SIMP and 2MASS observations span from 1 to 11 years, and the typical uncertainty of the calculated proper motions was 40 mas yr^{-1} .

2.2. Identifying Companions

For each target star, we calculated the proper motion of all sources within a radius of $4'$ and selected any source with a proper motion within 40 mas yr^{-1} of the target star as a candidate companion. Visual inspection was performed for all candidates to reject false detections of artifacts that are identified within catalogs as point sources. The available photometry from the 2MASS PSC catalog was then used to estimate a spectral type for each candidate companion (and target star when unknown). We also estimated a photometric distance and its uncertainty based on the J -band magnitude and the spectral type–magnitude relation of Hawley et al. (2002) when the information was not available in the literature. We required that the estimated distances of the target and can-

TABLE 1
PHOTOMETRIC DATA

Name	2MASS Name	α^a	δ^a	r'^b	i'^b	z'^b	J^a	H^a	K_s^a
NLTT 251 ^c	2MASS J00064746-0852350	00 ^h 06 ^m 47 ^s .47	-08° 52' 35.1''	17.30 ± 0.01	14.94 ± 0.01	13.73 ± 0.01	11.97 ± 0.02	11.43 ± 0.02	11.09 ± 0.02
...	2MASS J00064916-0852457	00 ^h 06 ^m 49 ^s .17	-08° 52' 45.7''	20.91 ± 0.05	18.26 ± 0.01	16.45 ± 0.01	14.14 ± 0.03	13.55 ± 0.03	13.13 ± 0.04
NLTT 687	2MASS J00140212-1814578	00 ^h 14 ^m 02 ^s .10	-18° 14' 58.0''	10.38 ± 0.02	9.81 ± 0.02	9.57 ± 0.02
...	2MASS J00135882-1816462	00 ^h 13 ^m 58 ^s .80	-18° 16' 46.2''	16.54 ± 0.14	15.89 ± 0.18	15.04 ± 0.13
NLTT 2274 ^d	2MASS J00415543+1341162	00 ^h 41 ^m 55 ^s .43	+13° 41' 16.2''	... g	15.42 ± 0.01	... g	10.16 ± 0.03	9.57 ± 0.03	9.35 ± 0.02
...	2MASS J00415453+1341351	00 ^h 41 ^m 54 ^s .53	+13° 41' 35.1''	21.15 ± 0.07	18.71 ± 0.01	16.83 ± 0.01	14.45 ± 0.03	13.67 ± 0.04	13.24 ± 0.03
BD-06 813	2MASS J04050271-0600261	04 ^h 05 ^m 02 ^s .71	-06° 00' 26.1''	... g	... g	... g	8.35 ± 0.02	7.93 ± 0.03	7.87 ± 0.03
...	2MASS J04050209-0600409	04 ^h 05 ^m 02 ^s .10	-06° 00' 40.9''	21.22 ± 0.06	18.54 ± 0.01	17.08 ± 0.01	15.11 ± 0.05	14.30 ± 0.05	13.88 ± 0.05
NLTT 20640 ^e	2MASS J08583671+2711068	08 ^h 58 ^m 36 ^s .72	+27° 11' 06.8''	15.92 ± 0.01	... g	13.50 ± 0.01	11.99 ± 0.02	11.40 ± 0.02	11.10 ± 0.01
...	2MASS J08583693+2710518	08 ^h 58 ^m 36 ^s .94	+27° 10' 51.8''	22.05 ± 0.11	19.45 ± 0.02	17.64 ± 0.02	15.05 ± 0.05	14.23 ± 0.05	13.66 ± 0.05
LSPM J1021+3704	2MASS J10215240+3704289	10 ^h 21 ^m 52 ^s .40	+37° 04' 29.0''	16.07 ± 0.01	... g	13.87 ± 0.01	12.43 ± 0.02	11.95 ± 0.02	11.76 ± 0.02
...	2MASS J10215386+3704166	10 ^h 21 ^m 53 ^s .87	+37° 04' 16.7''	24.67 ± 0.48	21.85 ± 0.14	19.91 ± 0.08	17.18 ± 0.03 ^f	16.25 ± 0.22	15.66 ± 0.23
...	2MASS J10432398-1706024	10 ^h 43 ^m 23 ^s .99	-17° 06' 02.4''	11.48 ± 0.02	10.89 ± 0.02	10.60 ± 0.03
...	2MASS J10432513-1706065	10 ^h 43 ^m 25 ^s .13	-17° 06' 06.6''	15.67 ± 0.06	15.07 ± 0.06	14.61 ± 0.11
NLTT 26746	2MASS J11150134+1606447	11 ^h 15 ^m 01 ^s .35	+16° 06' 44.7''	... g	16.61 ± 0.01	... g	11.14 ± 0.02	10.56 ± 0.02	10.32 ± 0.02
...	2MASS J11150150+1607026	11 ^h 15 ^m 01 ^s .50	+16° 07' 02.7''	22.94 ± 0.37	20.71 ± 0.07	18.59 ± 0.05	16.40 ± 0.12	15.22 ± 0.09	14.56 ± 0.11
NLTT 29392	2MASS J12024963+4204475	12 ^h 02 ^m 49 ^s .63	+42° 04' 47.5''	18.21 ± 0.01	... g	13.87 ± 0.01	12.43 ± 0.02	11.95 ± 0.02	11.67 ± 0.02
...	2MASS J12025009+4204531	12 ^h 02 ^m 50 ^s .09	+42° 04' 53.2''	21.45 ± 0.07	18.87 ± 0.01	16.96 ± 0.01	14.50 ± 0.03	13.69 ± 0.03	13.26 ± 0.03
LSPM J1259+1001	2MASS J12594217+1001407	12 ^h 59 ^m 42 ^s .17	+10° 01' 40.7''	17.76 ± 0.01	15.63 ± 0.00	14.44 ± 0.00	12.60 ± 0.02	12.03 ± 0.03	11.63 ± 0.02
...	2MASS J12594167+1001380	12 ^h 59 ^m 41 ^s .68	+10° 01' 38.0''	24.45 ± 0.76	21.58 ± 0.13	19.60 ± 0.10	16.72 ± 0.19	15.53 ± 0.14	14.89 ± 0.15
NLTT 36369	2MASS J14081918+3708294	14 ^h 08 ^m 19 ^s .19	+37° 08' 29.4''	15.60 ± 0.01	14.53 ± 0.01	13.48 ± 0.01	12.06 ± 0.02	11.45 ± 0.02	11.22 ± 0.02
...	2MASS J14081969+3708255	14 ^h 08 ^m 19 ^s .70	+37° 08' 25.6''	21.98 ± 0.10	19.09 ± 0.02	17.47 ± 0.02	15.42 ± 0.05	14.78 ± 0.06	14.35 ± 0.08
LSPM J1441+1856	2MASS J14412209+1856451	14 ^h 41 ^m 22 ^s .09	+18° 56' 45.1''	17.43 ± 0.04	... g	... g	11.44 ± 0.02	10.82 ± 0.03	10.55 ± 0.02
...	2MASS J14412565+1856484	14 ^h 41 ^m 25 ^s .65	+18° 56' 48.5''	23.38 ± 0.27	21.34 ± 0.07	19.41 ± 0.06	16.94 ± 0.18	16.17 ± 0.17	15.40 ± 0.13
NLTT 41701	2MASS J15590815+3735477	15 ^h 59 ^m 08 ^s .15	+37° 35' 47.7''	... g	... g	... g	9.12 ± 0.02	8.67 ± 0.02	8.56 ± 0.02
...	2MASS J15590740+3735275	15 ^h 59 ^m 07 ^s .40	+37° 35' 27.5''	22.89 ± 0.27	19.66 ± 0.03	18.07 ± 0.03	15.75 ± 0.07	14.92 ± 0.07	14.53 ± 0.08
HD 234344	2MASS J16460765+5020405	16 ^h 46 ^m 07 ^s .64	+50° 20' 41.1''	... g	... g	... g	7.62 ± 0.02	7.06 ± 0.02	6.97 ± 0.03
...	2MASS J16461148+5019456	16 ^h 46 ^m 11 ^s .48	+50° 19' 45.7''	20.47 ± 0.03	17.43 ± 0.01	16.66 ± 0.01	13.61 ± 0.02	12.98 ± 0.03	12.59 ± 0.02
HD 217246	2MASS J22591790+0806484	22 ^h 59 ^m 17 ^s .90	+08° 06' 48.4''	... g	... g	... g	8.56 ± 0.02	8.26 ± 0.03	8.19 ± 0.02
...	2MASS J22591631+0806556	22 ^h 59 ^m 16 ^s .31	+08° 06' 55.6''	21.83 ± 0.09	18.84 ± 0.01	17.61 ± 0.02	15.76 ± 0.06	15.14 ± 0.08	14.74 ± 0.10
NLTT 56936	2MASS J23274840+0451241	23 ^h 27 ^m 48 ^s .40	+04° 51' 24.2''	... g	... g	... g	8.16 ± 0.03	7.58 ± 0.05	7.41 ± 0.02
...	2MASS J23274947+0450583	23 ^h 27 ^m 49 ^s .48	+04° 50' 58.4''	21.54 ± 0.125	18.92 ± 0.02	17.17 ± 0.02	15.10 ± 0.03	14.36 ± 0.04	13.97 ± 0.05
TYC 1725-344-1	2MASS J23553113+1755239	23 ^h 55 ^m 31 ^s .14	+17° 55' 23.9''	... g	... g	... g	8.80 ± 0.03	8.38 ± 0.02	8.28 ± 0.02
...	2MASS J2355345+175404	23 ^h 55 ^m 34 ^s .50	+17° 54' 04.0''	23.24 ± 0.33	20.43 ± 0.04	18.73 ± 0.03	16.39 ± 0.12	15.42 ± 0.15	15.02 ± 0.15
NLTT 182	2MASS J00054143+0626256	00 ^h 05 ^m 41 ^s .43	+06° 26' 25.6''	17.08 ± 0.01	15.42 ± 0.04	14.51 ± 0.01	13.02 ± 0.03	12.51 ± 0.03	12.19 ± 0.03
...	2MASS J00054171+0626300	00 ^h 05 ^m 41 ^s .71	+06° 26' 30.1''	22.38 ± 0.16	19.86 ± 0.03	18.00 ± 0.02	15.81 ± 0.10	15.13 ± 0.11	14.62 ± 0.11
HD 2292	2MASS J00265848+1705088	00 ^h 26 ^m 58 ^s .49	+17° 05' 08.8''	8.88 ± 0.01	... g	... g	7.90 ± 0.027	7.55 ± 0.04	7.50 ± 0.03
...	2MASS J00265989+1704463	00 ^h 26 ^m 59 ^s .90	+17° 04' 46.4''	21.82 ± 0.13	19.16 ± 0.02	17.39 ± 0.02	15.40 ± 0.05	14.67 ± 0.05	14.39 ± 0.07
NLTT 4558	2MASS J01221872+0330470	01 ^h 22 ^m 18 ^s .72	+03° 30' 47.1''	... g	... g	... g	7.42 ± 0.02	7.14 ± 0.03	7.07 ± 0.02
...	2MASS J01221697+0331235	01 ^h 22 ^m 16 ^s .98	+03° 31' 23.6''	22.05 ± 0.13	19.95 ± 0.03	17.95 ± 0.03	15.47 ± 0.05	14.65 ± 0.06	14.40 ± 0.08
NLTT 30510	2MASS J12221994+3643539	12 ^h 22 ^m 19 ^s .94	+36° 43' 54.0''	... g	... g	... g	10.51 ± 0.02	9.98 ± 0.02	9.73 ± 0.02
...	2MASS J12221837+3643485	12 ^h 22 ^m 18 ^s .37	+36° 43' 48.5''	22.61 ± 0.17	20.21 ± 0.03	18.15 ± 0.03	15.97 ± 0.08	15.27 ± 0.09	14.85 ± 0.09
LSPM J1236+3000	2MASS J12363558+3000315	12 ^h 36 ^m 35 ^s .59	+30° 00' 31.6''	19.63 ± 0.02	17.75 ± 0.01	16.81 ± 0.01	15.28 ± 0.05	14.60 ± 0.06	14.30 ± 0.08
...	2MASS J12363647+3000315	12 ^h 36 ^m 36 ^s .48	+30° 00' 31.5''	23.04 ± 0.31	20.63 ± 0.05	18.86 ± 0.05	16.82 ± 0.20	16.06 ± 0.22	15.48 ± 0.20
NLTT 33793 ^d	2MASS J13205010+0955582	13 ^h 20 ^m 50 ^s .11	+09° 55' 58.3''	... g	... g	... g	7.89 ± 0.03	7.32 ± 0.04	7.22 ± 0.03
...	2MASS J13204159+0957506	13 ^h 20 ^m 41 ^s .59	+09° 57' 50.6''	20.40 ± 0.03	17.47 ± 0.01	15.80 ± 0.01	13.73 ± 0.03	13.08 ± 0.03	12.61 ± 0.03

^aData are from the 2MASS catalog (Cutri et al. 2003)

^bData are from the SDSS catalog (Ahn et al. 2012)

^cThis system has been identified to be a hierarchical triple system with an M6 primary and an M9+T5 secondary by Burgasser et al. (2012)

^dThis system has been identified as a binary by Faherty et al. (2010)

^eThis system has been identified as a binary by Zhang et al. (2010)

^fThis magnitude has been extracted from a CPAPIR MKO J-band image and has been converted to the 2MASS magnitude system. This object was poorly detected in the 2MASS catalog as it is faint.

^gSaturated

didate companion agree within the estimated uncertainties. Following this procedure, we identified 29 pairs of potential binary systems. We obtained imaging and spectroscopic follow-up observations of most of these candidates to improve their proper motion measurements and their spectral type determinations. We then applied a more detailed analysis, described below, to make a better assessment of their nature. Following this analysis, we found that 6 candidates systems are not comoving while 23 systems were found to be likely bound. These are the systems to be discussed in this paper (see Table 1).

Five of the 23 candidate pairs were found by other teams and reported as binary systems after we performed our initial search. The primary of these systems are NLTT 2274 (M4+M9.5), and NLTT 33793 (K4+M7.5), both found by Faherty et al. (2010), NLTT 20640 (Zhang et al. 2010, M4+L0), NLTT 251 (Burgasser et al. 2012, M7+M9+T5), and HD234344 (Mason et al. 2001a, K7,M7). In addition, shortly prior to the submission of this manuscript, a new study by Deacon et al. (2014) reported the discovery of 4 other of our systems : NLTT 4558 (G5+L1+T3), NLTT56936 (K5+M8), NLTT26746 (M4+L4) and NLTT30510 (M2+M9.5).

3. NEAR-INFRARED IMAGING

3.1. Observations

We obtained *J*-band observations of 14 candidate companions between 2012 November and 2013 May using the Observatoire du Mont Mégantic (OMM) wide field near-infrared camera, CPAPIR (Artigau et al. 2004), installed on the OMM 1.6 m telescope, and the OMM near-infrared spectro-imager SIMON (Albert 2006) installed on the CTIO 1.5 m telescope. The field of view (FOV) of CPAPIR at the OMM is $30' \times 30'$ with a pixel scale of $0.89'' \text{ pixel}^{-1}$, while the FOV of SIMON at the Cerro Tololo Inter-American Observatory (CTIO) 1.5 m is $8.4' \times 8.4'$ with a pixel scale of $0.49'' \text{ pixel}^{-1}$. Typically, the observations consisted of 15 individual exposures of 3 to 30 s, with a dither step of $2'$ between them. These observations provide a total time baseline of up to 15 years with respect to 2MASS for proper motion measurements.

3.2. Data Reduction

The reduction of the imaging data followed standard procedures. The images of SIMON and CPAPIR were sky subtracted using a median sky image constructed from the entire data set taken over the night in the *J* filter. The images were flat-fielded using a flat image derived from *on* and *off* dome images taken at the beginning or the end of the nights. Individual images astrometry was performed by cross-correlating point sources in the field with the 2MASS catalog. All images were then median-combined into a single science frame that was used for astrometric measurements.

3.3. Results

We measured the positions of the sources in our CPAPIR and SIMON follow-up imaging by finding all of the stars in the image and then fitting a 2D Gaussian over each one. These positions have been compared to those of all the objects in the 2MASS catalog that are up to $10'$ away from the target and the corresponding sources were associated. We determined the astrometric errors by computing the standard deviation of the difference between the positions in the CPAPIR/2MASS images and the corresponding positions in the 2MASS catalog propagated to the CPAPIR/SIMON epoch according to the proper motion listed in the NOMAD catalog (Zacharias et al. 2004); this was done for reference stars of brightness comparable to our targets. We determined the source positions in the SIMP data, also obtained with CPAPIR, in the same manner; those measurements are also given in Table 2 as they have not yet been published elsewhere.

For each candidate companion, we combined the position measurements from our follow-up imaging, 2MASS, SDSS, SIMP, and WISE to compute their proper motion using a weighted linear regression between the positions of the object and the measurement epochs. We adopted the uncertainty of the slope parameter as our uncertainty on the proper motion. The proper motions for all of our candidates, corrected for the parallax estimated from their photometric distance (see below), are compiled in Table 5. As an example, our calculated proper motions for all stars within $10'$ of NLTT 26746 are plotted on Figure 1 ; the common proper motion of our candidate compan-

TABLE 2
ASTROMETRIC MEASUREMENTS BASED ON OUR OBSERVATIONS

Name	RA (deg)	Uncertainty in RA (mas)	DEC (deg)	Uncertainty in DEC (mas)	Epoch (Reduced JD)	Source
2M1043-1706A	160.84974	340	-17.10118	400	54168.75	SIMP
	160.84956	560	-17.10128	670	56345.70	SIMON
	160.84953	130	-17.10125	130	56259.97	CPAPIR
2M1043-1706B	160.85452	340	-17.10234	400	54168.75	SIMP
	160.85435	220	-17.10245	110	56345.70	SIMON
	160.85433	250	-17.10240	130	56259.97	CPAPIR
2M1646+5019	251.54744	190	50.33065	190	55232.88	SIMP
	251.54735	400	50.33103	180	56330.86	CPAPIR
LSPM1259+1001	194.92540	860	10.02808	720	55232.91	SIMP
	194.92522	680	10.02804	270	56330.82	CPAPIR
2M1259+1001	194.92335	860	10.02741	720	55232.91	SIMP
	194.92339	320	10.02728	220	53900.55	CPAPIR
	194.92327	380	10.02737	270	56330.82	CPAPIR
LSPMJ1441+1856	220.34193	380	18.94546	390	55232.92	SIMP
	220.34189	160	18.94529	130	56330.89	CPAPIR
2M1441+1856	220.35673	380	18.94627	390	55232.92	SIMP
	220.37645	260	19.09413	290	56330.89	CPAPIR
NLTT182	1.42300	150	6.44028	170	53980.73	SIMP
2M0005+0626	1.42296	150	6.44028	170	53980.73	SIMP
	1.43611	360	6.51388	410	56619.50	SIMON
NLTT20640	134.65331	310	27.18477	350	55144.94	SIMP
	134.65344	120	27.18451	170	56329.48	CPAPIR
2M0858+2710	134.65424	310	27.18052	350	55144.94	SIMP
	134.67524	300	27.31993	340	56329.48	CPAPIR
NLTT33793	200.26834	190	10.02453	180	53838.67	SIMP
	200.26833	360	10.02452	280	56330.83	CPAPIR
2M1320+0957	200.17290	190	9.96377	180	53838.67	SIMP
	200.17247	110	9.96350	90	56330.83	CPAPIR
NLTT36369	212.07912	360	37.14177	250	55232.91	SIMP
	212.08075	330	37.14089	870	56330.80	CPAPIR
2M1408+3708	212.07911	360	37.14177	250	55232.91	SIMP
	212.08084	380	37.14090	390	56330.80	CPAPIR
NLTT41701	239.78411	470	37.59615	400	55232.89	SIMP
	239.78417	150	37.59600	160	56430.58	CPAPIR
2M1559+3735	239.78101	470	37.59051	400	55232.89	SIMP
	239.78105	120	37.59038	100	56430.58	CPAPIR
2M0122+0331	20.57078	210	3.52294	150	54036.68	SIMP
NLTT56936	352.02213	130	4.97526	170	53986.70	SIMP
	351.95329	290	4.85733	250	56572.54	SIMON
2M2327+0450	351.95691	130	4.84984	170	53986.70	SIMP
	351.95778	70	4.85024	290	56572.54	SIMON
2M0026+1704	6.74936	220	17.07940	280	53994.73	SIMP
BD-06813	61.26145	470	-6.00778	470	56349.54	SIMON
	61.26139	140	-6.00779	190	56258.78	CPAPIR
2M0405-0600	61.25892	180	-6.01190	180	56349.54	SIMON
	61.25890	110	-6.01187	110	56258.78	CPAPIR
NLTT2274	10.48038	360	13.68728	220	56619.54	SIMON
2M0041+1341	10.47664	140	13.69254	70	56619.54	SIMON
2M2355+1754	358.89345	360	17.90071	140	56619.54	SIMON
NLTT687	3.50881	1080	-18.24962	2160	56547.70	SIMON
2M0013-1816	3.49509	1080	-18.27954	2160	56547.70	SIMON
2M2259+0806	344.81841	140	8.11571	140	56570.54	SIMON
2M0006-0852	1.70457	250	-8.88072	220	56547.75	SIMON
LSPMJ1021+3704	155.46781	310	37.07414	70	56329.67	CPAPIR
2M1021+3704	155.47389	490	37.07081	190	56329.67	CPAPIR
NLTT26746	168.75463	130	16.11187	90	56329.69	CPAPIR
2M1115+1607	168.75524	220	16.11687	150	56329.69	CPAPIR
NLTT30510	185.58421	180	36.73147	110	56329.73	CPAPIR
2M1222+3643	185.57769	290	36.72998	300	56329.73	CPAPIR
LSPMJ1236+3000	189.14888	120	30.00824	110	56329.71	CPAPIR
2M1236+3000	189.15272	410	30.00832	210	56329.71	CPAPIR
2M1202+4204	180.70753	580	42.08037	640	56330.73	CPAPIR

ion with the primary is clearly seen.

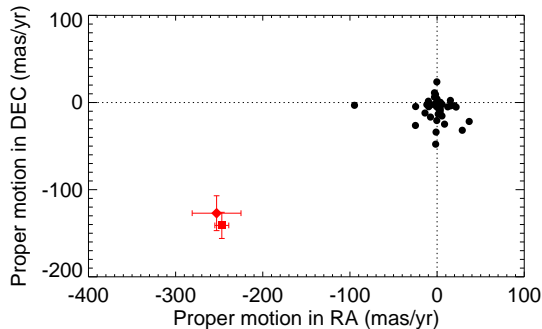


Fig. 1.— Proper motions for all objects within $10'$ of NLTT 26746 based on our follow-up imaging (2MASS, SDSS, CPAPIR, and WISE data). The proper motion of the candidate companion 2M1115+1607 is shown with a red diamond, while the proper motion of the primary star is shown with a red square. The two components of the candidate binary have proper motions consistent within the estimated uncertainties.

4. SPECTROSCOPY

4.1. Optical spectroscopy

We obtained optical spectroscopy follow-up observations of all candidates using the Gemini Multi-Object Spectrographs (GMOS) (Hook et al. 2004) at the Gemini South and North telescopes during semesters 2008A and 2008B (programs GN-2008A-Q-80, GN-2008A-Q-20, GS-2008A-Q-12, GS-2008B-Q-34, and GN-2008B-Q-107). We used a $1''$ wide slit, the R400 grating with OG515 blocking filter, and 2-pixel binning in both the spatial and the spectral direction. For each target, we obtained exposures with three central wavelength settings, 790 nm, 800 nm and 810 nm, to cover the small gaps between the three GMOS detectors. The exposure times range from 10s to 600s (see Table 3). We did not move the target in the slit during the observations. The resulting spectra have a resolving power of $R \sim 850$ and cover the wavelength range from 650 nm to 1000 nm. The typical seeing during the observations was $0.75''$ – $1.0''$. Standard calibrations were obtained for each science data set. We used the

calibration data of the G subdwarf LTT9239, the DA white dwarf EG 274 and the B0 star HZ44 for telluric and instrumental transmission calibration. Our main goal was to characterize the candidate companions, but given the short additional time needed, we also acquired a spectrum of the primary star during a visit to a given system. When the primary was not too bright to saturate the detector in an exposure of a few hundred seconds, both the primary and the companion were put in the slit simultaneously, otherwise a shorter observation of the primary was obtained after observation of the companion. Due to various issues during the execution of the observations, we were unable to procure data for all of the systems. In all, we obtained a spectrum for 14 candidate companions out for 23 and 10 candidate primaries out 23. A log of the observations is given in Table 3.

The GMOS spectroscopy data were reduced using a custom Interactive Data Language (*IDL*) routine. First, we corrected the individual exposures for the bias and flat field. We then extracted the spectral trace using a Moffat function extraction profile, allowing for a linear sky solution. We subsequently constructed a quadratic wavelength solution using calibration arc lamps, and corrected the spectra for wavelength-dependent instrumental transmission using a standard spectrum. The reference spectroscopic spectra were taken from Hamuy et al. (1994) and Massey et al. (1988). In the last step, we combined the individual spectra extracted from each of the 3 detector section, and finally combined all exposures together for a given object. The measurement uncertainties were estimated by extracting an empty sky region near the spectral trace, using the same method. All these spectra are normalized at $0.75 \mu\text{m}$. Figure 2 shows the GMOS spectra for 6 candidate primaries for which the spectral types were not published in the literature before this study. GMOS spectra at $R \sim 850$ of ten candidates are shown in Figure 3 and the remaining four are shown in Figure 4 with $R \sim 400$. The latter figure present the smoothed spectra our four faintest targets observed with GMOS. In all cases, a residual signal caused by an fringing effect from the detector is present. However, this effect affects the quality of our data significantly only for our faintest targets but even with this fringing, we are still able to identify the spectral type of the objects.

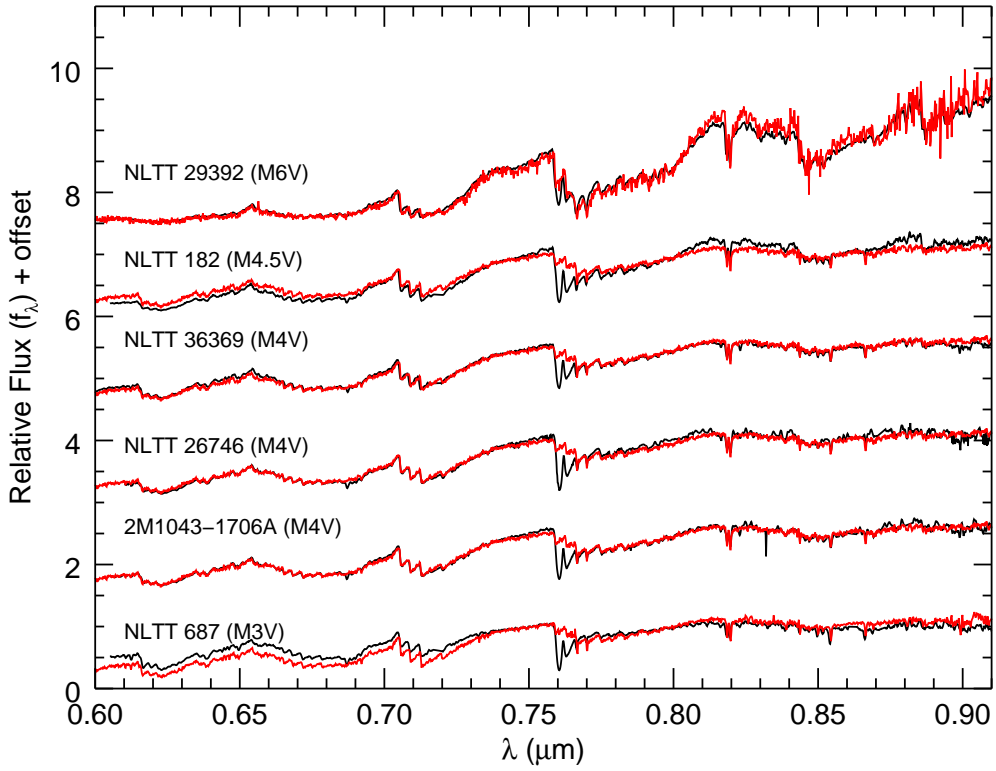


Fig. 2.— GMOS spectra of our 6 candidate primaries for which a spectral type was not available in the literature, displayed with a resolution of $R \sim 850$. The spectra are normalized at $0.75 \mu\text{m}$. As a comparison, we display in red the SDSS template spectra from Hawley et al. (2002) for the appropriate spectral type convolved to the same resolution. The feature in our spectra at $0.76 \mu\text{m}$ is telluric absorption that we did not correct.

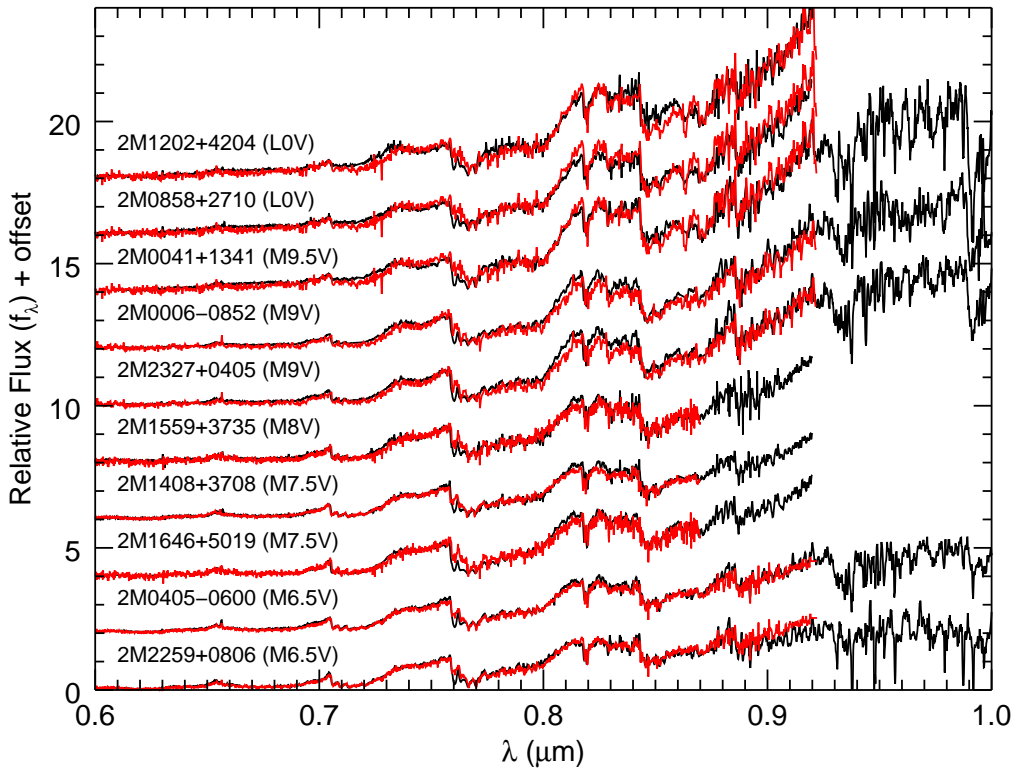


Fig. 3.— GMOS spectra of 10 of our candidate companions, displayed with a resolution of $R \sim 850$. The spectra are normalized at $0.75 \mu\text{m}$. As a comparison, we display in red the SDSS template spectra from Hawley et al. (2002) for the appropriate spectral type convolved to the same resolution. The feature in our spectra at $0.76 \mu\text{m}$ is telluric absorption that we did not correct. Different observation setups account for the different wavelength range.

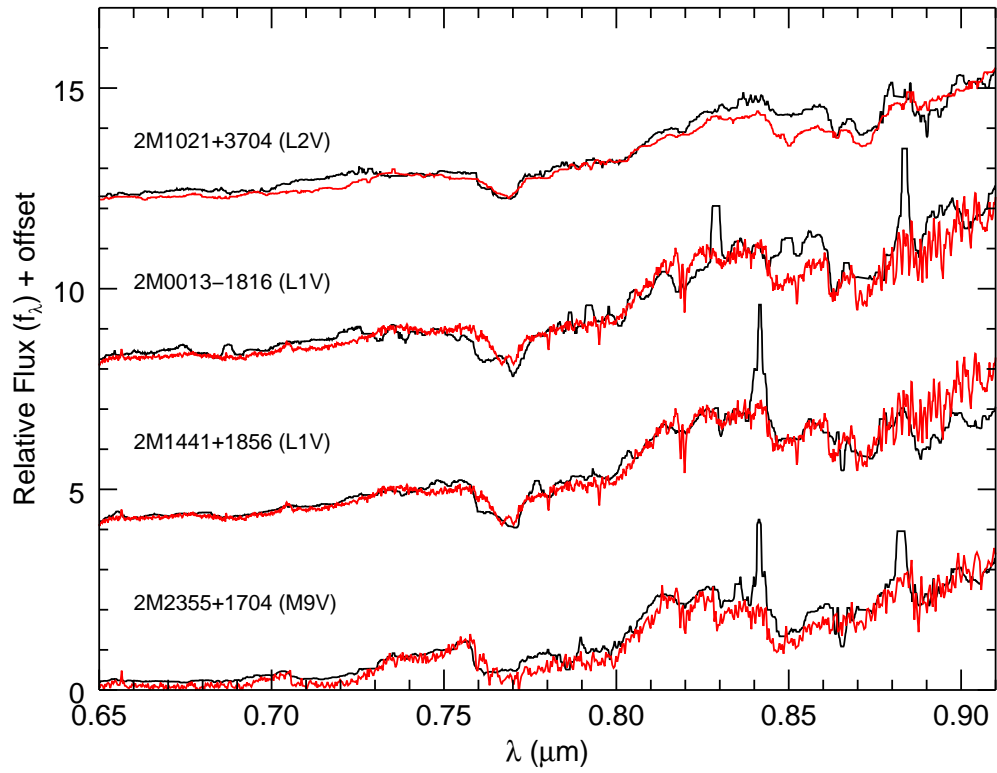


Fig. 4.— GMOS spectra of 4 of our candidate companions, displayed with a degraded resolution of $R \sim 400$ as these candidates were fainter and a lower signal-to-noise ratio was reached at full resolution. There is fringing in the data leading to a significant residual signal for these faint targets. The spectra are normalized at $0.75 \mu\text{m}$. As a comparison, we display in red the SDSS template spectra from Hawley et al. (2002) for the appropriate spectral type.

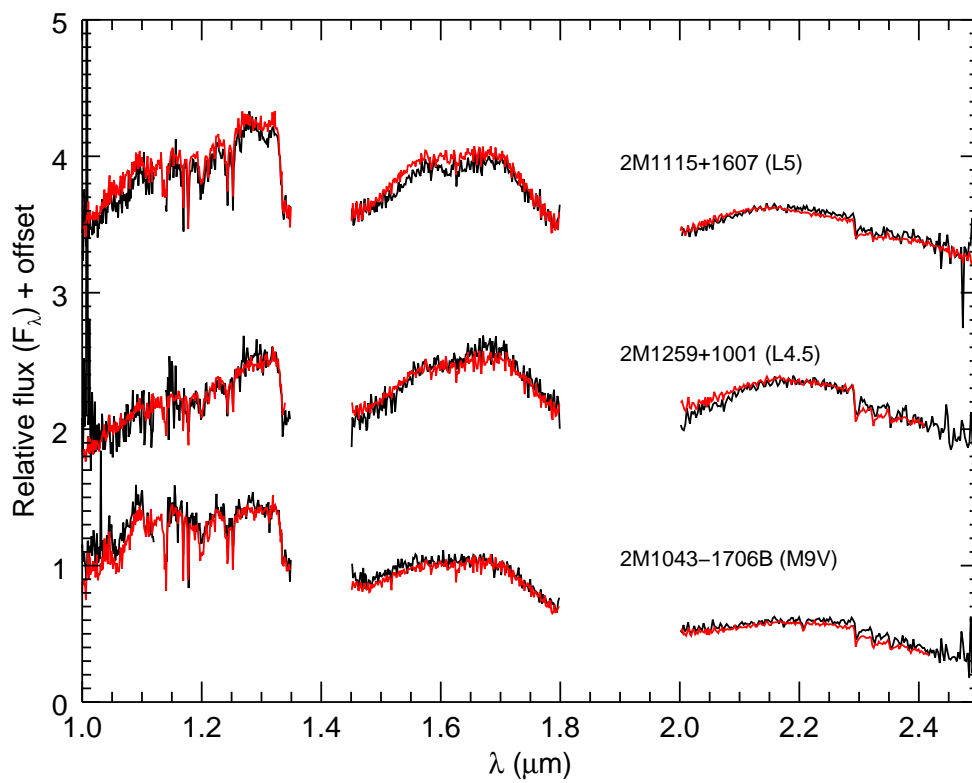


Fig. 5.— GNIRS spectra of 3 of our candidate companions, displayed with a spectral resolution of $R \sim 1700$. The spectra are normalized at $1.1 \mu\text{m}$. As a comparison, we display in red the spectra from SPEX IRTF Spectral Library (Cushing et al. 2005; Rayner et al. 2009) for the appropriate spectral type.

TABLE 3
GMOS AND GNIRS SPECTROSCOPIC OBSERVATIONS

System	Component	Obs. Date YYYY-MM-DD	Instrument	Number of exposures	Exp. time (s)	Standard
NLTT251	Both	2008-06-14	GMOS-S	6	600.	EG 274
NLTT 687	Primary	2008-06-15	GMOS-S	6	60.4	EG 274
	Companion	2008-06-15	GMOS-S	6	600.	EG 274
NLTT 2274	Primary	2008-08-05	GMOS-S	6	60.4	LTT 9239
	Companion	2008-08-05	GMOS-S	3	900.	LTT 9239
BD-06 813	Primary	2008-01-28	GMOS-S	6	60.4	EG 274
	Companion	2008-01-28	GMOS-S	6	600.	EG 274
NLTT 20640	Both	2008-02-11	GMOS-N	6	599.	HZ44
LSPM J1021+3704	Both	2008-02-27	GMOS-N	2	599.	HZ44
2M1043-1706	Primary	2008-01-28	GMOS-S	6	600.	HZ44
NLTT 26746	Primary	2009-01-01	GMOS-S	3	900.	LTT 9239
NLTT 29392	Both	2008-02-11	GMOS-N	6	599.	HZ44
NLTT 36369	Both	2008-04-14	GMOS-N	9	599.	HZ44
LSPM J1441+1856	Companion	2007-08-06	GMOS-S	10	600.	LTT 9239
NLTT 41701	Primary	2008-03-15	GMOS-N	6	9.99	HZ44
	Companion	2008-03-15	GMOS-N	9	599.	HZ44
HD 234344	Primary	2008-03-02	GMOS-N	6	29.9	HZ44
	Companion	2008-03-02	GMOS-N	9	419.	HZ44
HD 217246	Companion	2007-06-24	GMOS-S	6	600.	LTT9239
NLTT 56936	Companion	2008-12-27	GMOS-S	3	900.	LTT9239
TYC 1725-344-1	Companion	2007-06-21	GMOS-S	6	600.	LTT9239
NLTT 182	Primary	2008-06-30	GMOS-S	6	600.	EG 274
2M1043-1706	Companion	2007-04-01	GNIRS	8	120.	HD 137873
2M1115+1607	Companion	2007-01-08	GNIRS	11	60.0	HD 137873
2M1259+1001	Companion	2007-01-08	GNIRS	15	60.0	HD 137873

4.2. Near-Infrared Spectroscopy

Three of our candidate companions, 2M1043-1706B, 2M1115+1607, and 2M1259+1001, were identified on their own as brown dwarf candidates in a separate search for high proper motion brown dwarfs in the SIMP data (Artigau et al. 2009, Robert et al., in preparation), but have not yet been published. As other candidates identified in that search for brown dwarfs, they were followed-up using near-infrared spectroscopy with GNIRS at the Gemini South telescope in semester 2007A (GS-2007A-Q-28). We used a $0.3''$ wide slit, the 32 l mm^{-1} grating, the short camera, and the cross-dispersed mode for a resolving power of $R \sim 1700$ and a spectral coverage from $0.9 \mu\text{m}$ to $2.5 \mu\text{m}$. Observatory standard calibrations were obtained with each observation. For telluric and instrumental transmission calibration, the A0 star HD 137873 was observed shortly before/after each observation. The observations were obtained with a typical ABBA dither pattern along the slit with individual exposures of 60 to 120s with 8 to 15 exposures. The details of the observations are shown in Table 3.

The reduction of the spectra was made using custom (*IDL*) routines as described in Delorme et al. (2008). First, successive image pairs were subtracted to remove the sky emission and divided by a median combined spectral flat. They were

then corrected for both spectral and spatial distortions. To extract the spectra, a positive and a negative extraction box that matched the trace profile was used. An argon arc lamp spectrum was taken at the end of each sequence, which was used as a first wavelength calibration. The wavelength scale was then more precisely adjusted to the atmospheric OH lines (Rousselot et al. 2000). Finally, the spectra for each target extracted from image pairs were normalized and their median was taken to make the final spectra. The GNIRS spectra of the three companions are shown on Figure 5 along with a spectra from the SPEX IRTF Spectral Library (Cushing et al. 2005; Rayner et al. 2009)² corresponding to the same spectral type as determined below.

4.3. Results

We determined the spectral type of all objects observed with GMOS from spectral indices, and then confirmed them by visual comparison with templates. For each spectrum we computed the following spectral indices: PC3, PC4, and PC5 as defined by Martin et al. (1996) and Martín et al. (1999), TiO5 and VO from Cruz & Reid (2002), CaH, Ti I, and Ca II from Kirkpatrick et al. (1991), and VO 2 and TiO7 de-

²http://irtfweb.ifa.hawaii.edu/~spex/IRTF_Spectral_Library

finned by Lépine et al. (2003). Each of these indices constitutes a good spectral type indicator in some restricted spectral type interval, but altogether they cover the range from K5 to L6 dwarfs. The index values–spectral type relations and regimes of validity were taken from their respective papers. The measured indices are compiled in Table 4, along with the corresponding spectral types. The latter are averages of the spectral types obtained from all the indices that are valid for a given type. The few blanks in the table are caused by the shorter spectral coverage of some spectroscopic observations. We visually compared our spectra to templates from the Pickles Atlas (Pickles 1998) or to SDSS spectra of M and L dwarfs from Hawley et al. (2002) to confirm spectral typing. The spectral types of all companions observed with GMOS range from M6.5 to L1.

We determined the spectral type of the three companions observed with GNIRS using the spectral indices defined by Allers & Liu (2013), which are based on the H₂O, H₂O-1, H₂O-2, and H₂OD indices and which are valid for M5V to L7V dwarfs. Then, we visually compared our spectra to the templates of M and L dwarfs from the SPEX IRTF Spectral Library. We determined a spectral type of M9.0±0.5 for 2M1043-1706B, L5 ± 1 for 2M1115+1607, and L4.5 ± 0.5 for 2M1259+1001; these are indicated in Table 5.

There are 19 objects for which we do not have GMOS nor GNIRS observations. Among these are 10 primaries and 2 companions for which a spectral type was known from the literature and we adopted those values. For the remaining seven, we estimated a spectral type from their 2MASS and SDSS colors based on the color–spectral type relations of Sheppard & Cushing (2009). The spectral types adopted for all objects are summarized in Table 5. This table is divided in the two parts: the top half is for systems for which we have a spectrum for the companions while the lower half is for systems for which we did not have a spectrum for the companions.

For each object we estimated a photometric distance using their 2MASS *J*-band magnitude and the *M_J*-spectral type relations from Hawley et al. (2002) for late-K to M5 dwarfs, and from Dupuy & Liu (2012) for later type objects, M6 to L5. These distance estimates are given in Table 5.

5. PROBABILITY OF RANDOM ALIGNMENT

After determining the proper motion, the spectral types and the distance for all components, we need to confirm that they form a bound pair. The probability of random alignment is the probability that from chance, in a search like ours, we would find a physically unrelated companion star having the same proper motion and photometric distance as the primary, within our uncertainties, and that is separated by less than the observed separation of our candidate. This is given by the probability of finding two stars of the relevant spectral types within a given separation of each other and at the same distance, times the probability of finding two stars of the relevant spectral types with the same proper motion, given that they are at a similar location on the sky.

For the former probability, as our search targeted a fixed set of potential primary stars, we need only calculate the probability of finding a companion star close to those primaries. All of our candidate companions have spectral types in the M6–L5 range, thus this is the relevant range for statistical calculations. From the spatial density of M6–M8 dwarfs of $2.2 \times 10^{-3} \text{ pc}^{-3}$ per *I*-band magnitude interval determined by Phan-Bao et al. (2003) and the spatial density of M8–L3.5 of $1.64 \times 10^{-3} \text{ pc}^{-3}$ per *J*-band magnitude interval determined by Phan-Bao et al. (2008), we calculated the overall spatial density of late-M dwarfs to early-L dwarfs (M6 to L3.5). We used this density to calculate the number of such stars in a spherical shell of radius equal to the distance from the Sun to a candidate and thickness given by our distance estimate uncertainty. Then, from this number we calculated, the average number of stars in a sky projected disk of radius equal to the separation of our candidate binary, assuming an isotropic distribution of stars. We multiplied this number by 25 000, the number of primary stars targeted by our search, and finally calculated the corresponding probability of detecting at least one object within this total search area.

For the latter probability, we used Monte Carlo calculations to determine the proper motion distribution of stars of a given spectral type and at the sky position of the candidate system based on the observed Galactic space velocity (*UVW*) dis-

TABLE 4
SPECTRAL INDICES

Object	PC3 ^a	PC4 ^a	PC5 ^a	TiO5 ^b	VO ^b	CaH ^c	Ti I ^c	Ca II ^c	VO2 ^d	TiO7 ^d	Spectral Type ^e
NLTT251	1.3695	1.6816	1.7827	0.19484	2.1168	1.5603	1.0704	1.0764	0.56026	0.65387	M6 ± 0.5
2M0006-0852	2.3435	3.8938	4.8902	0.34909	2.3607	1.5009	1.0326	1.0677	0.32328	0.46659	M9 ± 0.5
NLTT687	1.0306	1.0248	0.93255	0.58126	2.0021	1.1914	1.0622	1.2380	0.89734	0.92856	M3 ± 0.5
2M0013-1816	2.8484	6.2637	7.3279	0.96672	2.3180	1.4236	1.0617	1.1923	0.60007	0.95069	L1 ± 0.5
NLTT2274	1.1037	1.1221	1.0918	0.40346	1.9970	1.2715	1.0803	1.1374	0.77698	0.85842	M4 ± 0.5
2M0041+1341	2.7069	4.6043	5.7158	0.68651	2.5128	1.3602	1.0093	1.0645	0.36967	0.62286	M9 ± 0.5
2M0405-0600	1.6339	2.3019	2.4712	0.26199	2.2343	1.3667	1.1098	1.1253	0.42198	0.57595	M6 ± 1
NLTT20640	1.1217	1.2361	...	0.37900	2.0244	1.3055	1.0679	1.1134	0.72927	0.85573	M4 ± 0.5
2M0858+2710	2.4959	4.7033	...	0.64835	2.3871	1.2406	0.98143	1.0637	0.38629	0.65786	L0 ± 1
LSPMJ1021+3704	1.0898	1.1628	...	0.38845	1.9939	1.2819	1.0796	1.1583	0.75780	0.88121	M4 ± 0.5
2M1021+3704	2.7920	5.3320	...	1.0516	0.46435	0.92451	...	1.0668	0.60661	0.66820	L2
2M1043-1706A	1.0665	1.1986	1.1118	0.41786	1.9828	1.2421	...	1.1573	0.77439	0.87779	M4 ± 0.5
NLTT26746	1.0896	1.0664	1.1495	0.44003	1.9733	1.2758	1.1094	1.1651	0.83645	0.85031	M4 ± 0.5
NLTT29392	1.3948	2.0186	...	0.21082	2.1644	1.4311	1.0827	1.0974	0.49018	0.65474	M6 ± 0.5
2M1202+4204	2.7094	5.3242	...	0.66899	2.4729	1.3948	0.96756	1.0718	0.39638	0.70797	L0 ± 0.5
NLTT36369	1.0359	1.0841	...	0.42531	2.0007	1.2596	1.0741	1.1489	0.80273	0.89932	M4 ± 0.5
2M1408+3708	1.6805	2.5229	...	0.22558	2.3573	1.4836	1.0556	1.1543	0.37181	0.57255	M7 ± 0.5
2M1441+1856	2.7019	4.2794	2.7264	0.88903	2.2368	1.5198	0.75043	1.2276	0.50723	0.76976	L1 ± 1
2M1559+3735	1.8393	2.9506	...	0.27357	2.4630	1.3777	1.0318	1.1406	0.33012	0.55086	M8 ± 0.5
2M1646+5019	2.0450	3.0980	...	0.17044	2.1751	1.8641	1.0559	1.1482	0.39253	0.54864	M7 ± 0.5
2M2259+0806	1.5610	1.8795	1.6930	0.14590	2.1279	1.5757	1.0905	1.2289	0.50888	0.61669	M6 ± 0.5
2M2327+0405	2.1572	3.2263	3.8603	0.27870	2.4432	1.4433	1.0444	1.0839	0.33743	0.49614	M9 ± 0.5
2M2355+1754	2.2927	3.7816	2.9846	0.42313	2.4953	1.3452	1.0084	1.1327	0.40961	0.76501	M9 ± 0.5
NLTT182	1.1426	1.2647	1.1793	0.34680	2.0167	1.3121	1.0885	1.1310	0.69285	0.79268	M4.5 ± .5

^aThe spectral indice is from Martin et al. (1996)

^bThe spectral indice is from Cruz & Reid (2002)

^cThe spectral indice is from Kirkpatrick et al. (1991)

^dThe spectral indice is from Lépine et al. (2003)

^eThe spectral types shown in the last column are the median of the spectral types computed using the spectral indices presented in the table.

tributions of stars in the solar neighborhood. The *UVW* distributions were derived from the velocity dispersions given by Mikami & Heck (1982) for F, G and K stars, by Bochanski et al. (2011) for M dwarfs, and by Schmidt et al. (2010) for L dwarfs. We then determined the probability that a star of the spectral class of the primary and a star of the spectral class of the secondary, at the sky position of the system, would have proper motions larger than 0.1 mas yr^{-1} and consistent with each other within 2σ .

We finally multiplied the above two probabilities to get the probability of random alignment; the results are given in Table 5. For all of our candidate systems, this probability is less than 1.3×10^{-3} , indicating that they most likely form a physical pairs.

6. DISCUSSION

We estimated the mass of the companions in our systems based on evolution models; this requires first estimating an age for the systems. The tangential velocity of our systems, which is an indicator of the population to which an object belongs, has been compared to the Besançon Galac-

tic model (Robin et al. 2003). All of our systems have tangential velocities consistent with being part of the thin disk. According to the Galactic model simulations, most of our targets have a $> 80\%$ probability to be younger than 3 to 5 Gyr. We also looked for sign of youth in our GNIRS spectra. We used the spectral indices defined by Allers & Liu (2013), already used to compute the spectral types, which are also sensitive to surface gravity. According to these indices, none of the three companions have low surface gravity. We then looked for $H\alpha$ emission, at 656.3 nm , which is indicative of the stellar activity and moderately correlated with age (West et al. 2008). Visual inspection of the spectra and calculations of the $H\alpha$ equivalent widths indicate that 2M0405-0600 (M6.5), 2M1202+4204 (L0) and 2M1043B (M9) have equivalent widths higher than 1 \AA , and are thus active. Schmidt et al. (2010) had already identified that NLTT 29392B was an active L0 dwarf. However, this does not mean that they are particularly young as M dwarfs can be active during a few Gyr (see discussion in West et al. (2008))

³See <http://www.vlbinaries.org/> for an up-to-date census of the known very low mass binaries, maintained by N. Siegler, C. Gelino and A. Burgasser.

TABLE 5
DERIVED PARAMETERS FOR THE BINARY SYSTEMS

Name	Spectral type ^a	$\mu_{\alpha} \cos \delta$ (mas/yr)	μ_{δ} (mas/yr)	Separation (μ)	Distance ^b (pc)	Prob ^c	P. sep. (AU)	Pos. angle (deg)	Mass ^d (M_{\odot})
NLTT 251 ^P	M6.0 ± 0.5	-70 ± 9	-311 ± 6	27.4 ± 0.6	25 ⁺⁷ ₋₁₁	2.8 × 10 ⁻⁵	850 ⁺⁸⁴ ₋₁₅₂	113 ± 1	0.102–0.133
2M0006-0852	M9.0 ± 0.5	-59 ± 18	-318 ± 9		37 ⁺⁵ ₋₁₁				0.079–0.085
NLTT 687	M3.0 ± 0.5	-44 ± 12	-173 ± 5	118.1 ± 0.6	42 ⁺²⁶ ₋₁₆	3.9 × 10 ⁻⁴	7400 ⁺¹¹⁶⁰ ₋₁₂₅₀	203.1 ± 0.3	0.389–0.412
2M0013-1816	L1.0 ± 0.5	-20 ± 41	-212 ± 37		83 ⁺⁷ ₋₂₇				0.072–0.078
NLTT 2274 ^f	M4.0 ± 0.5	-165 ± 56	-155 ± 2	23.2 ± 0.8	23 ⁺¹⁴ ₋₉	1.6 × 10 ⁻⁴	725 ⁺²³⁰ ₋₂₅₃	325 ± 2	0.207–0.272
2M0041+1341	M9.5 ± 0.5	-162 ± 58	-153 ± 13		40 ⁺⁶ ₋₁₂				0.076–0.083
BD-06 813	K0 ^o	31 ± 8	-139 ± 5	17.4 ± 0.2	68 ± 10 ^h	7.6 × 10 ⁻⁴	1340 ⁺¹⁰² ₋₃₄₀	211.6 ± 0.5	0.925–1.014
2M0405-0600	M6.5 ± 1	42 ± 6	-117 ± 10		86 ⁺² ₋₃₇				0.096–0.114
NLTT 20640 ^l	M4.0 ± 0.5	103 ± 5	-179 ± 5	15.6 ± 0.2	54 ⁺³² ₋₂₀	2.2 × 10 ⁻⁵	780 ⁺²⁶³ ₋₂₇₀	168.9 ± 0.6	0.207–0.272
2M0858+2710	L0 ± 1	104 ± 7	-182 ± 6		48 ⁺³ ₋₁₄				0.074–0.081
LSPM J1021+3704	M4.0 ± 0.5 ^h	-132 ± 9	-141 ± 4	22.2 ± 0.4	88 ⁺³⁹ ₋₁₃	1.3 × 10 ⁻³	3000 ⁺⁶⁵⁰ ₋₆₇₅	125 ± 1	0.207–0.272
2M1021+3704	L0 ± 1	-131 ± 8	-124 ± 12		93 ⁺¹³ ₋₃₆				0.071–0.076
2M1043-1706A	M4.0 ± 0.5	-97 ± 16	-140 ± 22	17.1 ± 0.1	42 ⁺²⁶ ₋₁₆	7.1 × 10 ⁻⁴	1020 ⁺²⁸⁸ ₋₃₀₆	84 ± 0.5	0.207–0.272
2M1043-1706B	M9.0 ± 0.5	-90 ± 14	-141 ± 22		75 ⁺⁶ ₋₂₃				0.079–0.085
NLTT 26746 ^u	M4.0 ± 0.5	-247 ± 8	-141 ± 2	18.0 ± 0.2	36 ⁺²² ₋₁₄	1.5 × 10 ⁻⁴	660 ⁺²¹⁶ ₋₄₄₁	6.5 ± 0.7	0.207–0.272
2M1115+1607	L5 ± 1 ^t	-253 ± 28	-127 ± 20		37 ⁺³ ₋₃₅				0.056–0.073
NLTT 29392	M6.0 ± 0.5	-306 ± 11	-300 ± 17	7.3 ± 0.1	33 ⁺² ₋₁₆	1.1 × 10 ⁻⁵	310 ⁺¹⁶ ₋₁₃₅	42.0 ± 0.8	0.102–0.133
2M1202+4204	L0.0 ± 0.5	-292 ± 6	-276 ± 11		38 ⁺² ₋₁₁				0.074–0.081
LSPM J1259+1001	M5 ± 1 ^g	-142 ± 15	22 ± 9	7.65 ± 0.08	42 ⁺⁴ ₋₂₁	2.9 × 10 ⁻³	345 ⁺¹⁹⁶ ₋₁₅₆	250.9 ± 0.6	0.121–0.167
2M1259+1001	L4.5 ± 0.5	-146 ± 5	29 ± 7		47 ⁺⁵ ₋₁₈				0.057–0.074
NLTT 36369	M4.0 ± 0.5	-247 ± 8	80 ± 1	7.9 ± 0.1	55 ⁺³³ ₋₂₁	9.3 × 10 ⁻⁵	590 ⁺¹⁶² ₋₁₈₀	122 ± 1	0.207–0.272
2M1408+3708	M7.5 ± 0.5	-249 ± 1	80 ± 10		84 ⁺⁴ ₋₂₉				0.087–0.096
LSPM J1441+1856	M6 ^h	-56 ± 9	-154 ± 9	51.1 ± 0.2	56 ⁺³⁷ ₋₁₀	8.7 × 10 ⁻⁴	4110 ⁺¹²¹⁹ ₋₁₁₆₆	86.4 ± 0.2	0.102–0.133
2M1441+1856	L1 ± 1	-59 ± 9	-185 ± 12		99 ⁺¹⁰ ₋₃₄				0.072–0.079
NLTT 41701	K2 ^h	42 ± 12	-137 ± 9	22.4 ± 0.5	(61 ⁺⁶¹ ₋₂₇) ⁱ	8.1 × 10 ⁻⁴	1735 ⁺⁶⁹⁰ ₋₆₄₄	204 ± 1	0.872–0.941
2M1559+3735	M8.0 ± 0.5	46 ± 9	-152 ± 14		89 ⁺⁶ ₋₂₉				0.084–0.090
HD 234344 ^s	K7 ^h	-129 ± 29	394 ± 11	69.3 ± 0.3	31.6 ± 0.9 ^m	2.4 × 10 ⁻⁴	2700 ⁺¹⁵⁸ ₋₅₉₃	146.2 ± 0.3	0.705–0.751
2M1646+5019	M7.5 ± 0.5	-118 ± 4	400 ± 7		36 ⁺³ ₋₄				0.087–0.095
HD217246	G5 ^h	137 ± 34	59 ± 19	24.7 ± 0.2	(68 ⁺⁷⁰ ₋₃₂) ⁿ	3.6 × 10 ⁻⁴	2340 ⁺¹¹²⁵ ₋₁₀₀₀	286.0 ± 0.5	0.821–0.930
2M2259+0806	M6.5 ± 0.5	122 ± 6	69 ± 5		121 ⁺²⁰ ₋₅₁				0.096–0.113
NLTT 56936 ^u	K2+K5 ⁿ	443 ± 1	171 ± 8	30.3 ± 0.1	64 ± 9 ^k	4.7 × 10 ⁻⁵	1825 ⁺¹⁸⁰ ₋₃₉₀	147.8 ± 0.2	1.46±0.09 ⁿ
2M2327+04505	M9 ± 0.5	443 ± 6	191 ± 12		57 ⁺³ ₋₁₇				0.079–0.085
TYC 1725-344-1	G5III ⁿ	-65 ± 21	-78 ± 14	93.8 ± 0.4	(40 ⁺²⁵ ₋₁₅) ⁱ	2.8 × 10 ⁻⁴	6700 ⁺¹⁸⁰⁵ ₋₂₄₇₀	149.0 ± 0.23	1.91±0.11 ⁿ
2M2355+1754	M9.0 ± 0.5	-69 ± 16	-86 ± 3		103 ⁺¹⁰ ₋₃₇				0.079–0.085
NLTT 182	M4.5 ± 0.5	213 ± 6	-113 ± 7	6.1 ± 0.1	62 ⁺³⁸ ₋₂₃	1.4 × 10 ⁻⁴	400 ⁺¹²⁶ ₋₁₃₅	43 ± 4	0.157–0.181
2M0005+0626	L0 ± 1 ^g	205 ± 7	-126 ± 8		69 ⁺⁵ ₋₂₂				0.079–0.085
LSPM J1236+3000	M6 ± 1 ^g	140 ± 5	-124 ± 4	12.2 ± 0.8	112 ⁺⁶ ₋₅₂	1.9 × 10 ⁻³	1580 ⁺¹⁵⁶ ₋₆₂₄	89 ± 4	0.102–0.133
2M1236+3000	M9.0 ± 1 ^g	162 ± 27	-102 ± 15		126 ⁺¹⁸ ₋₄₄				0.079–0.085
HD 2292	G5 ^r	-143 ± 15	-113 ± 19	30.5 ± 0.5	(42 ⁺²⁸ ₋₁₄) ⁿ	2.6 × 10 ⁻⁴	1200 ⁺¹⁸⁰ ₋₅₁₀	138 ± 1	1.05–1.12
2M0026+1704	M9 ± 1 ^g	-149 ± 2	-128 ± 41		65 ⁺⁴ ₋₂₀				0.108–0.118
NLTT 30510 ^u	M3 ± 1 ^g	269 ± 12	-39 ± 16	20.7 ± 0.5	45 ⁺⁷ ₋₂₃	1.9 × 10 ⁻⁴	1635 ⁺⁶⁴⁸ ₋₃₈₄	254.2 ± 0.9	0.377–0.431
2M1222+3643	L0 ^e	272 ± 18	-36 ± 8		70 ± 10 ^l				0.074–0.081
NLTT 33793 ^j	K5 ^j	-210 ± 64	-131 ± 12	168.5 ± 0.3	(38.1 ^{+2.6} _{-2.3}) ^j	5.4 × 10 ⁻⁵	5780 ⁺²⁰⁴⁰ ₋₁₁₉₀	311.7 ± 0.1	0.724–0.782
2M1320+0957	M8 ^j	-222 ± 38	-141 ± 10		36 ± 3 ^j				0.087–0.096
NLTT 4558 ^u	G5 ^m	22 ± 13	-142 ± 15	44.8 ± 0.8	(58 ± 3 ^k)	3.5 × 10 ⁻⁵	2222 ⁺³⁰⁸ ₋₉₆₀	324.2 ± 1	1.05–1.12
2M0122+0331	L2 ± 1 ^g	45 ± 10	-162 ± 5		43 ⁺¹³ ₋₄₀				0.071–0.076

^aSpectral type are extracted from our GMOS or GNIRS spectra unless noted otherwise, ^b Distance computed using the spectral types and the relations from Dupuy & Liu (2012) and Hawley et al. (2002), ^c Probability of random alignment, ^d Masses are evaluated using the mass– M_J relation from the BT-Settl model of Allard (2014), ^e Zhang et al. (2009a), ^f This system has been identified as a M4+L0 binary by Faherty et al. (2010). Their spectral types, proper motions, distance and separation are consistent with the ones we found, ^g Spectral type calculated from i'-J' (Sheppard & Cushing 2009), ^h Pickles & Depagne (2010), ⁱ Ammons et al. (2006) has estimated a distance that matches to one obtained from the spectral type extracted from the optical GMOS spectrum, ^j This system has been identified as a M4+L0 binary by Faherty et al. (2010), ^k Heliocentric distance from Anderson & Francis (2013), ^l Photometric distance from Zhang et al. (2009a), ^m Heliocentric distance from Anderson & Francis (2013), ⁿ Hrivnak et al. (1995), ^o The spectral type is from Barney (1951), ^p This system has been identified to be a hierarchical triple system with an M7.0±0.5 primary and an M8.5±0.5+T5±1 secondary by Burgasser et al. (2012). Their proper motions, distance and separation are consistent with the ones we found, ^q This system has been identified as a M4+L0 binary by Zhang et al. (2010). Their spectral types, proper motions, distance and separation are consistent with the ones we found, ^r Kharchenko (2001), ^s This system has been identified as a K7+M7 binary by Mason et al. (2001a). Their spectral types, proper motions, distance and separation are consistent with the ones we found, ^t Zhang et al. (2009b) found a spectral type of L1 by colors and has identified it as a brown dwarf candidate, ^u This system has been identified by Deacon et al. (2014), ^v The mass of NLTT 4558 has been calculated by Porto de Mello et al. (2014)

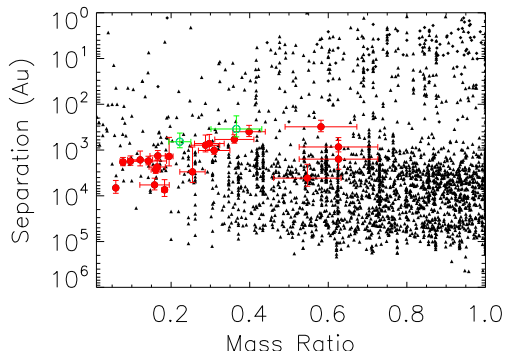


Fig. 6.— Separation (in AU) versus mass ratio for our systems and for known binaries. The red circles represent our sample. The LSPMJ1259+1001 system and the NLTT26746 system, for which the companion is either a L4.5 or a L5 dwarf, are shown with the open green circle. Very low mass binaries from the Very Low Mass Binaries Archive³ are shown as a diamond while the triangles represent binary systems from Gomes et al. (2013) and references therein, Janson et al. (2012), Dhital et al. (2010), Faherty et al. (2010) and references therein, Raghavan et al. (2010), Metchev & Hillenbrand (2004), Reid et al. (2001), Wilson et al. (2001), Mason et al. (2001b), Reid & Gizis (1997), Fischer & Marcy (1992), and Close et al. (1990).

on the relatively weak constraint that H α provides for an individual object).

In addition, we used the BANYAN II code (Gagné et al. 2014) to test if any of our targets belong to a nearby young moving group. We found out that while most of our target have a higher probability of belonging to the field, one of them (NLTT182) has a 98.8% probability of being a Beta Pictoris member, with a corresponding false positive rate of 4.5%. This is quite interesting but by no means a proof of youth or true membership; the complete 3D kinematics would have to be confirmed, as well as youth from various indicators. We only have an optical spectrum of the primary star of this system, and we looked for gravity-sensitive spectroscopic indices in it (Kirkpatrick et al. 2000; Cruz & Reid 2002; Cruz et al. 2007; Reid et al. 2008), such as the Na-a index, the Na-b index, the K-a index, and the

CrH-a index, to assess whether this object is young or not. However, these four indices fall close to the field scatter and the result of our analysis is mainly inconclusive. More observations will be necessary to firmly establish whether or not this system is young. For the purpose of this paper, due to the lack of solid evidence, we simply assume this system to be of the age of the field, as we do for all of our other systems.

Based on the above analyses, we thus estimated that the ages of all of the systems are roughly 1–7 Gyr. We then evaluated the masses using the mass– M_J relation from the BT-Settl model of Allard (2014), where the M_J are obtained from our inferred spectral types using the relation of Hawley et al. (2002) and Dupuy & Liu (2012). In the cases where the distance were not well defined, we decided to use the effective temperature instead of the J magnitude to find the masses. The effective temperature for each target has been extracted from its spectral type according to the relations in Pecaut & Mamajek (2013). We note that masses inferred in this manner are overestimated by about 10% for objects with a G or early-K spectral types as compared to Henry & McCarthy (1993). The estimated masses for ages between 1 to 7 Gyr are given in Table 5. The uncertainties come from the propagation of the error of spectral types on the inferred magnitudes (or effective temperatures).

Figure 6 shows the separation in AU of our systems as a function of their mass ratio, as compared with other known binaries. Some of our new systems, having low mass ratios, reach a sparsely populated regions of the diagram. In particular, we found 14 systems with a mass ratio less than 0.3, below the bulk of the previously known population.

As some of our system have a low binding energy, it is interesting to find out if the systems are stable. Orbital evolution is possible for wide, weakly bound binaries and it might lead to their disruption as they travel through the Galaxy and encounter stars and giants molecular clouds. Weinberg et al. (1987) worked out the calculations for the evolution and lifetimes of such wide binary systems in the solar neighbourhood; these can easily be scaled to very low-mass stars as was done by Artigau et al. (2007). For all of our binaries, we find that the half-life is of the order of a Hubble

time or larger. The probability of survival is thus high for all systems.

Burgasser et al. (2005) have shown that the binary fraction is higher for ultra cold dwarfs that are in a wide binary system where the primary is a stellar object. Furthermore, Whitworth & Stamatellos (2006) discussed the possibility that H₂ dissociation might trigger a secondary fragmentation of a companion low-mass protostar if the latter is at the cooler outer parts of the circumstellar disk (> 100 AU) and is spinning at a high enough rate. Thus, it is possible that some of our companions (and perhaps primaries) are unresolved binaries themselves. If that were the case, this could be reconciled with our common photometric distance estimates given the large associated uncertainties and could be tested observationally with either adaptive optics observations or high-precision radial-velocity monitoring of the primary.

To differentiate the evolutionary states of our stars, we use the four spectral classes of metallicity defined by Lépine et al. (2007) that are defined by the $\zeta_{TiO5/CaH}$ index, which is based on the CaH2, CaH3 and TiO5 molecular bands in the optical. This index has been re-calibrated by Dhital et al. (2012) and is used to differentiate dwarfs, subdwarfs, extreme subdwarfs and ultrasubdwarfs. Using this index for all of our M dwarfs, we found that they all have $\zeta_{TiO5/CaH} > 0.85$, meaning that they all are in the dwarf metallicity class with near-solar metallicity.

7. CONCLUSION

We have discovered 14 new binary systems with companions of spectral types M6–L5 at separations of 6''–170'' from their primaries, corresponding to projected separations of 250–7500 AU at the distances of the systems. We also recovered nine already known binaries. Ten of our companions have a spectral type of L0 or later, two of them being comfortably in the brown dwarf regime: 2M1115+1607 (L5±1) and 2M1259+1001 (L4.5±0.5). The latter is a newly identified brown dwarf and orbits a mid-M dwarf. The most widely separated system is NLTT 687, consisting of an M3+L1 pair with a separation of 7400 AU. Other very wide systems are TYC 1725-344-1, a G5+M9 pair with a separation of 6700 AU and

LSPMJ1441+1856, a M6+L1 pair with a separation of 4110 AU. Pairs consisting of a G-type star and an ultracool dwarf (e.g., HD21746, G5+M6.5) provide an opportunity to calibrate the metallicity scale of M ultracool dwarfs Rojas-Ayala et al. (2010). This calibration is useful because determining the metallicity of such M dwarfs would normally require parallaxes and high-resolution spectra, which are expensive data to acquire and are limited to a few bright cool stars. While our systems are not the most extremes, they can nevertheless help better define the parameter space in which wide low-mass companions can form.

We thank our referee, Eric Mamajek, for excellent suggestions that improved the quality of this paper. This research has made use of the SIMBAD database, operated at CDS, Strasbourg, France and of the VizieR catalogue access tool, CDS, Strasbourg, France. This publication makes use of data products from the Two Micron All Sky Survey, which is a joint project of the University of Massachusetts and the Infrared Processing and Analysis Center/California Institute of Technology, funded by the National Aeronautics and Space Administration and the National Science Foundation. This publication makes use of data products from the Wide-field Infrared Survey Explorer, which is a joint project of the University of California, Los Angeles, and the Jet Propulsion Laboratory/California Institute of Technology, funded by the National Aeronautics and Space Administration. This research has benefited from the M, L, T, and Y dwarf compendium housed at DwarfArchives.org. This publication has made use of the Very-Low-Mass Binaries Archive housed at <http://www.vlmbinaries.org> and maintained by Nick Siegler, Chris Gelino, and Adam Burgasser. This research has benefited from the SpeX Prism Spectral Libraries, maintained by Adam Burgasser at <http://pono.ucsd.edu/~adam/browndwarfs/spexprism>.

REFERENCES

- Adelman-McCarthy, J. K., Agüeros, M. A., Allam, S. S., et al. 2008, *The Astrophysical Journal Supplement Series*, 175, 297
- Ahn, C. P., Alexandroff, R., Allende Prieto, C., et al. 2012, *The Astrophysical Journal Supplement Series*, 203, 21
- Albert, L. 2006, Ph.D. Thesis, 13
- Allard, F. 2014, in , 271–272, 00000

- Allers, K. N., & Liu, M. C. 2013, *The Astrophysical Journal*, 772, 79
- Ammons, S. M., Robinson, S. E., Strader, J., et al. 2006, *The Astrophysical Journal*, 638, 1004
- Anderson, E., & Francis, C. 2013, *VizieR Online Data Catalog*, 5137, 0
- Artigau, E., Doyon, R., Vallee, P., Riopel, M., & Nadeau, D. 2004, in , 1479–1486
- Artigau, É., Lafrenière, D., Doyon, R., et al. 2007, *The Astrophysical Journal Letters*, 659, L49
- Artigau, É., Lafrenière, D., Doyon, R., et al. 2009, in *American Institute of Physics Conference Series*, Vol. 1094, 15th Cambridge Workshop on Cool Stars, Stellar Systems, and the Sun, ed. E. Stempels, 493–496
- Barney, I. 1951, *Transactions of the Astronomical Observatory of Yale University*, 23, 1, 00000
- Bochanski, J. J., Hawley, S. L., & West, A. A. 2011, *The Astronomical Journal*, 141, 98
- Bonfils, X., Delfosse, X., Udry, S., et al. 2005, *Astronomy and Astrophysics*, 442, 635
- Burgasser, A. J., Kirkpatrick, J. D., & Lowrance, P. J. 2005, *The Astronomical Journal*, 129, 2849
- Burgasser, A. J., Luk, C., Dhital, S., et al. 2012, *The Astrophysical Journal*, 757, 110
- Close, L. M., Richer, H. B., & Crabtree, D. R. 1990, *The Astronomical Journal*, 100, 1968
- Cruz, K. L., & Reid, I. N. 2002, *The Astronomical Journal*, 123, 2828
- Cruz, K. L., Reid, I. N., Kirkpatrick, J. D., et al. 2007, *The Astronomical Journal*, 133, 439
- Cushing, M. C., Rayner, J. T., & Vacca, W. D. 2005, 623, 1115
- Cutri, R. M., & et al. 2012, *VizieR Online Data Catalog*, 2311, 0
- Cutri, R. M., Skrutskie, M. F., van Dyk, S., et al. 2003, *VizieR Online Data Catalog*, 2246, 0
- Deacon, N. R., Liu, M. C., Magnier, E. A., et al. 2014, *ArXiv e-prints*, arXiv:1407.2938
- Delorme, P., Delfosse, X., Albert, L., et al. 2008, *Astronomy and Astrophysics*, 482, 961, 00101
- Dhital, S., West, A. A., Stassun, K. G., & Bochanski, J. J. 2010, *The Astronomical Journal*, 139, 2566
- Dhital, S., West, A. A., Stassun, K. G., et al. 2012, *The Astronomical Journal*, 143, 67
- Duchêne, G., & Kraus, A. 2013, arXiv:1303.3028 [astro-ph]
- Dupuy, T. J., & Liu, M. C. 2012, *The Astrophysical Journal Supplement Series*, 201, 19
- Epchtein, N., Deul, E., Derriere, S., et al. 1999, *Astronomy and Astrophysics*, 349, 236
- Faherty, J. K., Burgasser, A. J., Bochanski, J. J., et al. 2011, *The Astronomical Journal*, 141, 71
- Faherty, J. K., Burgasser, A. J., West, A. A., et al. 2010, *The Astronomical Journal*, 139, 176
- Fischer, D. A., & Marcy, G. W. 1992, *The Astrophysical Journal*, 396, 178
- Gagné, J., Lafrenière, D., Doyon, R., Malo, L., & Artigau, É. 2014, *ApJ*, 783, 121
- Gomes, J. I., Pinfield, D. J., Marocco, F., et al. 2013, *Monthly Notices of the Royal Astronomical Society*, 431, 2745
- Hamuy, M., Suntzeff, N. B., Heathcote, S. R., et al. 1994, *Publications of the Astronomical Society of the Pacific*, 106, 566
- Hawley, S. L., Covey, K. R., Knapp, G. R., et al. 2002, *The Astronomical Journal*, 123, 3409
- Henry, T. J., & McCarthy, Jr., D. W. 1993, *AJ*, 106, 773
- Hook, I. M., Jørgensen, I., Allington-Smith, J. R., et al. 2004, *Publications of the Astronomical Society of the Pacific*, 116, 425, 00290
- Hrivnak, B. J., Guinan, E. F., & Lu, W. 1995, *The Astrophysical Journal*, 455, 300
- Janson, M., Hormuth, F., Bergfors, C., et al. 2012, *The Astrophysical Journal*, 754, 44
- Kharchenko, N. V. 2001, *Kinematika i Fizika Nebesnykh Tel*, 17, 409
- Kirkpatrick, J. D., Henry, T. J., & McCarthy, D. W. 1991, *The Astrophysical Journal Supplement Series*, 77, 417
- Kirkpatrick, J. D., Reid, I. N., Liebert, J., et al. 2000, *AJ*, 120, 447
- Lawrence, A., Warren, S. J., Almaini, O., et al. 2007, *Monthly Notices of the Royal Astronomical Society*, 379, 1599
- Lépine, S. 2005, *The Astronomical Journal*, 130, 1680
- Lépine, S., Rich, R. M., & Shara, M. M. 2003, *The Astronomical Journal*, 125, 1598
- . 2007, *The Astrophysical Journal*, 669, 1235
- Martín, E. L., Delfosse, X., Basri, G., et al. 1999, *The Astronomical Journal*, 118, 2466
- Martin, E. L., Rebolo, R., & Zapatero-Osorio, M. R. 1996, *The Astrophysical Journal*, 469, 706
- Mason, B. D., Wycoff, G. L., Hartkopf, W. I., Douglass, G. G., & Worley, C. E. 2001a, *The Astronomical Journal*, 122, 3466
- . 2001b, *The Astronomical Journal*, 122, 3466
- Massey, P., Strobel, K., Barnes, J. V., & Anderson, E. 1988, *The Astrophysical Journal*, 328, 315
- Metchev, S. A., & Hillenbrand, L. A. 2004, in , 238
- Meyer, M. R., Adams, F. C., Hillenbrand, L. A., Carpenter, J. M., & Larson, R. B. 2000, *Protostars and Planets IV*, 121
- Mikami, T., & Heck, A. 1982, *Publications of the Astronomical Society of Japan*, 34, 529
- Pecaut, M. J., & Mamajek, E. E. 2013, *ApJS*, 208, 9
- Phan-Bao, N., Crifo, F., Delfosse, X., et al. 2003, *Astronomy and Astrophysics*, 401, 959

- Phan-Bao, N., Bessell, M. S., Martín, E. L., et al. 2008, *Monthly Notices of the Royal Astronomical Society*, 383, 831
- Pickles, A., & Depagne, É. 2010, *Publications of the Astronomical Society of the Pacific*, 122, 1437
- Pickles, A. J. 1998, *Publications of the Astronomical Society of the Pacific*, 110, 863
- Porto de Mello, G. F., da Silva, R., da Silva, L., & de Nader, R. V. 2014, *Astronomy & Astrophysics*, 563, A52
- Radigan, J., Lafrenière, D., Jayawardhana, R., & Doyon, R. 2009, *The Astrophysical Journal*, 698, 405
- Raghavan, D., McAlister, H. A., Henry, T. J., et al. 2010, *The Astrophysical Journal Supplement Series*, 190, 1
- Rayner, J. T., Cushing, M. C., & Vacca, W. D. 2009, *The Astrophysical Journal Supplement Series*, 185, 289
- Reid, I. N., Cruz, K. L., Kirkpatrick, J. D., et al. 2008, *AJ*, 136, 1290
- Reid, I. N., & Gizis, J. E. 1997, *The Astronomical Journal*, 114, 1992
- Reid, I. N., Gizis, J. E., Kirkpatrick, J. D., & Koerner, D. W. 2001, *The Astronomical Journal*, 121, 489
- Robin, A. C., Reylé, C., Derrière, S., & Picaud, S. 2003, *Astronomy and Astrophysics*, 409, 523
- Rojas-Ayala, B., Covey, K. R., Muirhead, P. S., & Lloyd, J. P. 2010, *The Astrophysical Journal Letters*, 720, L113
- Rousselot, P., Lidman, C., Cuby, J.-G., Moreels, G., & Monnet, G. 2000, *Astronomy and Astrophysics*, 354, 1134
- Salim, S., & Gould, A. 2003, *The Astrophysical Journal*, 582, 1011
- Schmidt, S. J., West, A. A., Hawley, S. L., & Pineda, J. S. 2010, *The Astronomical Journal*, 139, 1808
- Sheppard, S. S., & Cushing, M. C. 2009, *The Astronomical Journal*, 137, 304
- Weinberg, M. D., Shapiro, S. L., & Wasserman, I. 1987, *The Astrophysical Journal*, 312, 367
- West, A. A., Hawley, S. L., Bochanski, J. J., et al. 2008, *The Astronomical Journal*, 135, 785
- Whitworth, A. P., & Stamatellos, D. 2006, *Astronomy and Astrophysics*, 458, 817
- Wilson, J. C., Kirkpatrick, J. D., Gizis, J. E., et al. 2001, *The Astronomical Journal*, 122, 1989
- Zacharias, N., Monet, D. G., Levine, S. E., et al. 2004, 36, 1418
- Zhang, Z. H., Pokorny, R. S., Jones, H. R. A., et al. 2009a, *Astronomy and Astrophysics*, 497, 619
- . 2009b, *Astronomy and Astrophysics*, 497, 619
- Zhang, Z. H., Pinfield, D. J., Day-Jones, A. C., et al. 2010, *Monthly Notices of the Royal Astronomical Society*, 404, 1817